TISSUE ENGINEERING: Part A
Volume 16, Number 9, 2010

DOI: 10.1089/ten.tea.2009.0595

Tissue-Engineered Three-Dimensional *In Vitro* Models for Normal and Diseased Kidney

Balajikarthick Subramanian, B.S.,[1,2] Darya Rudym, B.S.,[1,3] Chris Cannizzaro, Ph.D.,[1] Ronald Perrone, M.D.,[3] Jing Zhou, M.D., Ph.D.,[4] and David L. Kaplan, Ph.D.[1]

Morphogenesis of epithelial cells involves processes by which kidney shape and function are regulated. The lack of *in vitro* models that are sustainable for longer time periods and emulating complex intercellular interactions of the kidney have limited understanding about epithelial tissue morphogenesis and its aberrations in diseases such as autosomal dominant polycystic kidney disease (ADPKD). A sustainable three-dimensional (3D) coculture system for normal and diseased kidney tissues is reported here. Tubule- and ADPKD cyst-derived cells were cultured in extracellular matrix molecules infused into 3D porous silk scaffolds, and these cultures were subsequently extended into a perfusion bioreactor. The results indicated collagen–matrigel-mediated morphogenesis for both (normal and disease) cell types and also supported coculturing with fibroblasts. The structural and functional features of the kidney-like tissue structures were validated based on the distribution of E-cadherin, N-cadherin, Na^+ K^+ ATPase pump, and cellular uptake of the organic anion (6-carboxy fluorescein). Further, the structures were sustained for longer time periods using a perfusion bioreactor to demonstrate the potential utility of this 3D *in vitro* coculture system for ADPKD research, other epithelial tissue systems, and for *in vitro* drug screening.

Introduction

Morphogenesis of epithelial cells *in vivo* is a complex phenomenon involving cues from extracellular matrix (ECM) molecules, solute concentration gradients, and mechanical inputs from fluid-flow-induced stress.[1,2] Current advanced *in vitro* approaches such as organotypic explant cultures, cellular spheroids, microcarrier culture, and three-dimensional (3D) gel culture provide some relevant complexity of the *in vivo* system.[3,4] However, a more robust method of culturing cells for extended function for months while mimicking *in vivo* features remains a need. Moreover, in 3D diseased tissue models, it is essential to recapitulate abnormalities of the tissue and also to show systematic analysis both at the cellular and molecular levels to relate the *in vitro* system to *in vivo* pathology. It has been suggested that a tissue engineering approach to develop organ or tissue mimics by employing scaffolds and reactor systems would be optimal for developing such models to investigate physiology or pathophysiology *in vitro*.[5]

Autosomal dominant polycystic kidney disease (ADPKD) is one of the most common genetic diseases that involve tubular epithelial structures of the kidney.[6,7] The disease is characterized by the progressive formation of focal cysts in tubular segments of nephrons causing bilateral kidney enlargement.[6,7] Expansion of cysts and extensive interstitial fibrosis associated eventually lead to kidney failure.[6,7] ADPKD is caused by mutations in either of the two genes encoding plasma membrane-spanning Pkd1 (polycystin-1) and Pkd2 (polycystin-2), together accounting for >95% of the cases.[6,7] The polycystins are known to regulate several processes, including cell cycle, mechanosensation, and migration.[8–10] Studies have also shown the association of polycystin-1 with several signaling pathways, including mammalian Target of Rapamycin, Phospho-Inositol-3-Kinase (PI3k/Akt), and Wnt.[10–12] Gene knockout studies of polycystin-1 have shown abnormalities in tubule development of kidneys and other organs.[13] In addition, stromal cell types such as fibroblasts or adipocytes can modulate the morphogenesis of kidney tubules.[14]

Animal models developed to investigate the pathophysiology of ADPKD have provided important clues about the role of cell proliferation, alterations in basement membrane, vectorial transport in cystic epithelium, and aberrations in stromal cells leading to cystic enlargement and interstitial fibrosis.[6,7,15] However, variations in animal models and

[1]Department of Biomedical Engineering, Tufts University, Medford, Massachusetts.
[2]Biomedical Engineering and Biotechnology Program, University of Massachusetts Lowell, Lowell, Massachusetts.
[3]Division of Nephrology, Tufts Medical Center, Tufts University School of Medicine, Boston, Massachusetts.
[4]Renal Division, Brigham and Women's Hospital, Harvard Medical School, Boston, Massachusetts.

technical challenges for systemic analysis leave the events causing cyst initiation and role of PKD genes in the process undefined.[16] There has been increased interest for *in vitro* models with more complexity and with relevance to *in vivo* systems as an alternate to traditional two-dimensional (2D) cultures and to animal models, to address the limitations above. These *in vitro* systems would be useful for the study of the disease origins and be useful for drug screening, bridging the gap between 2D cell culture models and *in vivo* models of ADPKD.[17]

To develop a 3D kidney tissue model system, the biomaterial scaffolds should provide appropriate morphology, structure, and chemistry to support the cell interactions as well as tissue structure and function. Matrix molecules such as collagen or matrigel provide some structural support and important matrix-mediated cell signaling. Silk fibroin scaffolds provide the porous features for transport, have robust mechanical properties, and retain size and open porous structures for extended time frames due to the slow biodegradation.[18] These features are critical to establishing long-term culture systems for the tissue engineering goals outlined above.

Therefore, in the present study we employed silk-based porous scaffolds with collagen–matrigel content, and a perfusion reactor system to generate 3D kidney tissue models. We report for the first time, the recapitulation of functional kidney tubules and cysts that could be maintained for longer time frames (>2 weeks). Further, the tissue models developed offer relevant *in vivo*-like complexities from the ECM components, solute gradients from interstitial cells such as fibroblasts, and fluid flow induced shear stress.

Materials and Methods

Cell culture

Mouse embryonic kidney (MEK) epithelial cells derived from different tubular segments of nephrons of $Pkd1^{+/+}$ (normal) and $Pkd1^{null/null}$ (disease) mice, immortalized by temperature-sensitive SV-40 large T antigen, were provided by Jing Zhou (Harvard Medical School).[13] Cells were maintained in permissive conditions at 33°C and 5% CO_2 in high-glucose Dulbecco's minimum essential medium (DMEM) (Invitrogen) supplemented with 10% fetal bovine serum (Invitrogen), 3 U/mL of interferon-γ (Sigma), 15 μg/mL ITS liquid medium supplement (Sigma), 36 ng/mL hydrocortisone (Sigma), 10^{-7} U/L triiodo-L-thyronine (Sigma), and 1% penstrep (Invitrogen). All epithelial cell culture experiments were initiated after differentiating the cells for at least 5 days in nonpermissive conditions at 37°C and without interferon-γ. Immunoblot analysis showed the reduction in T-antigen protein after 5 days of preculture (Supplemental Fig. S1, available online at www.liebertonline.com/ten). Mouse fibroblasts (ATCC: CCL-163) from BALB/3T3 clone A31 embryo were cultured in high-glucose DMEM (Invitrogen) supplemented with 10% fetal bovine serum (Invitrogen) and 1% penstrep (Invitrogen).

Silk scaffolds

Aqueous silk scaffolds were prepared from silk fibroin solution extracted from *Bombyx mori* as we have previously described.[19] Briefly, 2 mL of 7% aqueous silk solution was mixed with 4 g of sodium chloride beads (Sigma), with particle sizes within the range of 850–1000 μm, in a cylindrical Teflon container and allowed to dry for 48 h at room temperature. Containers were washed in distilled water for 2 days to dissolve the sodium chloride, and the resulting scaffolds were removed from the container and excised using an 8-mm biopsy punch (Acuderm Inc.). The final dimensions of the scaffolds were 8×4 mm (diameter×height).

Cell seeding

For matrigel-infused scaffold experiments, epithelial cells were mixed with growth-factor-reduced matrigel (BD Biosciences) and added to the scaffolds. The pores of the scaffolds were filled with matrix and allowed to gel for 30 min at 37°C. Cells were mixed with matrigel to a final concentration of 2×10^5 cells/mL. Similarly, for collagen–matrigel-infused scaffold experiments, a 1:1 mix of collagen and matrigel was filled in the pores of scaffolds. The final concentration of collagen in the scaffolds was 1 mg/mL for all groups. Coculture experiments were initiated in collagen–matrigel-infused scaffolds with equal amounts of each cell type and maintained in a combined medium (1:1) of epithelial and fibroblast medium types.

Immunoblotting

Cells were lysed in radio-immunoprecipitation assay (RIPA) buffer (Pierce Biotechnology) with Halt protease inhibitor (Pierce Biotechnology) at 4°C for 30 min, and the total cell lysates were centrifuged at 14,000 rpm for 15 min to recover the soluble protein fractions from the supernatant. The protein concentration in each sample was evaluated using Bradford assay (Bio-Rad), and equal amounts of proteins from samples were electrophoresed in 4%–10% bis-tris gel (Invitrogen) after heating at 70°C for 10 min in Nupage LDS sample buffer (Invitrogen). The proteins were then transferred to a polyvinylidenefluoride membrane (Invitrogen) and probed with antibodies after blocking with 3% skimmed milk (Bio-Rad). Beta actin (Abcam) (1:1000) and SV40 T-antigen (Abcam) (1:1000) were probed with mouse monoclonal antibody and goat anti-mouse horseradish peroxidase conjugate (Santa Cruz Biotechnology) (1:2000).

Scanning electron microscopy

Samples were fixed in 2.5% glutarldehyde in 0.1 M sodium cacodylate, pH 7.3. After rinsing, they were postfixed in 1% osmium tetroxide in 0.1 M sodium cacodylate buffer and dehydrated with graded ethanol solutions. Critical point drying of samples was done in Samdri 790 with liquid CO_2 and was mounted on aluminum stubs with gold/palladium sputter coating. Images were collected with a ISI-DS-130 instrument (Focused Resolutions) with digital camera.

Flow cytometry analysis

Proliferation of fibroblasts was analyzed using trace carboxyfluorescein diacetate succinimidyl ester (CFSE) cell proliferation kit (C34554; Molecular Probes). Briefly, cells were seeded in collagen–matrigel-infused silk scaffolds after labeling with 25 μM Carboxyfluorescein diacetate, succirimidyl ester (CFSE) reagent and allowed to proliferate for 2 weeks. The cells were extracted from the scaffolds with

collagenase I (Sigma) digestion, followed by 0.25% trypsin–ethylenediaminetetraacetic acid (Invitrogen) and were run in a FACS Calibur System (BD Biosciences). For 2D systems, cells were cultured in sub-confluent conditions for 7 days. Unlabeled cells were used to set flow cytometry parameters as a control population and 2-week samples were compared with 48 h samples to evaluate proliferation. Results were analyzed using Flow Jo software (Treestar).

Histology and fluorescence imaging

Formalin-fixed 5-μm scaffold sections were deparraffinized and stained for hematoxylin and eosin as described previously.[19] For immunofluorescence 5-μm sections were deparaffinized and antigen retrieval was performed with antigen unmasking solution (Vector Laboratories) by boiling slides for 30 min. After antigen retrieval, scaffold sections were blocked with 5% bovine serum albumin (BSA) supplemented with 10% serum from the secondary antibody host, in Dulbecco's phosphate-buffered saline (Invitrogen). E-cadherin was probed with rabbit polyclonal (1:50; Abcam) and goat polyclonal to rabbit IgG-Cy5 conjugate (1:200; Abcam). N-cadherin was probed with mouse monoclonal (1:50; Abcam) and goat polyclonal to mouse IgG-FITC conjugate (1:100; Abcam). Na^+ K^+ ATPase was probed with mouse monoclonal and goat polyclonal to mouse IgG-FITC conjugate (1:100; Abcam). Slides were counterstained for the nucleus using 4′,6′-diamidino-2-phenylindole (DAPI) (Invitrogen) and mounted with fluoroguard antifade reagent (Bio-Rad).

Whole scaffold imaging for actin staining of fibroblasts was carried out after 3% paraformaldehyde fixation and permeabilization of the samples in 0.1% Triton X-100 (Sigma) for 30 min at 4°C, followed by blocking with 3% BSA. Samples were probed for F-actin and the nucleus using phalloidin-alexa 488 (1:50) (Invitrogen) and propidium iodide (PI) (Invitrogen), respectively. Briefly, scaffolds were incubated with phalloidin diluted with 3% BSA at 37°C for 1 h followed by PI diluted with 3% BSA for 15 min. All fluorescence images were collected using Leica DM IRE2 confocal microscope system.

Organic anion transport

Scaffolds were incubated in phenol red free plain DMEM for 30 min, followed by addition of organic anion 6-carboxy fluorescein (6-CF) (Sigma) and PI (Invitrogen) for 45 min. For drug responsive groups, cells were incubated with 2 mM organic anion transport (OAT) inhibitor, probenecid (Sigma) along with 6-CF and PI for 45 min. After uptake, scaffolds were washed with PBS three times and imaged for live cells by confocal microscopy.

Perfusion reactor system

The perfusion reactor system contains wells (8 mm diameter) that are custom designed to accommodate the scaffolds. The wells are directly connected to a peristaltic pump through perfusion tubing arising from the bottom of wells. The chamber is closed with a lid with four slits to which the other end of perfusion tubing is connected. The peristaltic pump is connected to a flow-rate-controlling unit. All experiments were done with a flow rate of 0.3 mL/min, which leads to linear velocity of 71.8 μm/s across the scaffolds.

Morphometric and statistical analyses

Three arbitrarily chosen fields in histology sections were examined at 10× magnification and the number of structures was counted. Branching and tubule structures were counted together in normal cells and compared with structures in disease cells. For quantification of perfusion culture results, the average number of structures (cyst and tubules) from three sections of each scaffold (a total of four scaffolds) was used. Statistical analyses were carried out using GraphPad Instat software. Data were analyzed using one-way analysis of variance, and when statistical significance was seen by analysis of variance, the Student–Newman-Keuls separation of means was used to find group differences. Statistical significance was set at minimal value of $p < 0.05$, and all values are expressed as mean ± standard error of the mean.

Results

Morphogenesis of kidney epithelial cells

ECM proteins play a significant role in mediating the cystogenesis and tubulogenesis of kidney epithelial cells. Therefore, we attempted to optimize an ECM component suitable to infuse in scaffolds and mediate 3D culture. Previous studies with 3D gel culture showed mixed reports for type I collagen in mediating the morphogenesis of cyst-derived epithelial cells (disease cells).[20,21] Normal kidney epithelial cells such as Madin-Darby Canine Kidney cells (MDCK) cells develop polarized cyst and form branching structures with hepatocyte growth factor (HGF) treatment and develop into tubular structures in collagen.[1,22] Our results indicated that collagen alone did not mediate morphogenesis of cyst-derived cells in scaffolds (Fig. 1D). However, matrigel and collagen–matrigel mediated the formation of small cystic structures (Fig. 1E, F). In contrast, both collagen and matrigel mediated morphogenesis of tubule-derived epithelial cells (normal cells) (Fig. 1A, B) and supported branching upon treatment with HGF (data not shown). Further, morphogenesis was observed for normal cells in collagen–matrigel-infused scaffolds resulting in cystic structures, with a quantitatively significant population of cells showing spontaneous branching (Fig. 1C). Taken together, these results suggest that collagen–matrigel was a suitable matrix to mediate the morphogenesis of both MEK cell types in silk scaffolds and also provide a platform for the inclusion of stromal cell types such as fibroblasts. In addition, the loss of gene function in disease cells altered morphogenetic properties related to ECM content, consistent with prior reports.[1,20]

Fibroblast coculture

The morphogenesis of epithelial cells is known to be influenced by stromal interactions.[14] Moreover, plasticity of matrix molecules is also influenced by cells such as fibroblasts.[23] Consequently, it was of interest to include fibroblasts in the 3D kidney tissue systems. Results from actin staining indicated that fibroblasts exhibited morphologies as pro-migratory types with dendritic extensions or as bipolar morphologies and were evenly distributed in collagen–matrigel matrices (Fig. 2A–C). Flow cytometric analysis of fibroblasts in the collagen–matrigel scaffolds indicated minimal proliferation after 2 weeks in comparison with day 2 samples (Fig. 2D). Further, coculture of fibroblasts

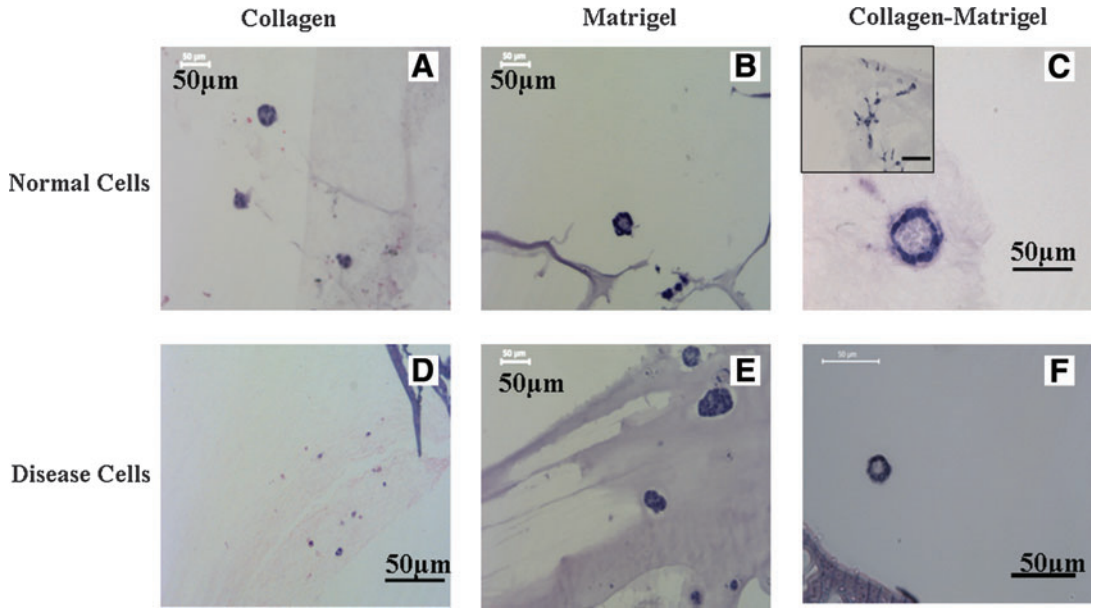

FIG. 1. Effect of extracellular matrix molecules in mediating morphogenesis. (**A–F**) H&E images. (**A–C**) Normal cells. (**D–F**) Disease cells. (**A, D**) Collagen-infused in scaffolds. (**B, E**) Matrigel-infused in scaffolds. (**C, F**) Collagen–matrigel-infused in scaffolds. The inner image in (**C**) shows branching structures, while the images (**A–C, E, F**) show cystic structures with lumen. (**D**) shows lack of any structures. Culture was static; time was 2 weeks. Scale bar in µm. H&E, hematoxylin and eosin. Color images available online at www.liebertonline.com/ten.

modulated the morphogenesis of the normal epithelial cells, with more tubule-like structures and branching structures formed (Fig. 2E, $p < 0.01$), while it did not change the morphogenetic pattern of the disease cells (Fig. 2E–H). These results indicate that the *pkd1* gene is essential for fibroblast-induced branching.

Morphology scaffolds

The morphology of the aqueous-derived scaffolds with and without the infused collagen–matrigel was evaluated by scanning electron microscopy (SEM) (Fig. 3A, B). The scaffolds without collagen–matrigel displayed interconnected networks of pores with rough surfaces. The pores sizes were heterogeneous in nature, ranging between 850 and 1000 µm. In contrast, the scaffolds infused with collagen–matrigel but without cells showed interstices filled with gel (Fig. 3B). Also from the image it is evident that the gels did not contract and were thus compatible with the silk scaffolds. The collagen–matrigel-infused scaffolds with cells displayed a major change in morphology (Fig. 3C, D), likely due to the remodeling or contraction of matrix components by the cells. Further, the morphogenesis of the cells did result in a separation of the silk scaffolds from the matrix, allowing the interface to remain intact (Fig. 3C, D).

Disease tissue

It is known that *in vivo* cells exhibit asymmetric polarized organization, whereas abnormalities in polarity and transition from reabsorptive to secretory phenotype have been observed in ADPKD.[1,6] In the present study we evaluated asymmetric polarity via the distribution of characteristic proteins such as E-cadherin, N-cadherin, and Na^+ K^+ ATPase pump, while comparing with kidney tissue samples as controls (Fig. 4A–D). E-cadherin was basolaterally distributed in the normal cells, while weak diffuse cytoplasmic localization was seen in the disease cells, similar to normal and disease kidney samples. N-cadherin was weakly dispersed in the cytoplasm for both normal and disease cells, while localized to the membrane in the disease kidney and almost absent in the normal kidney. We also evaluated the distribution of the Na^+ K^+ ATPase pump, which is associated with reabsorptive functions of kidney tubules, while a lack of this function is associated with the disease.[21] The results showed basolateral distribution for normal cells and the loss of this feature in the disease cells, in accordance with normal tissue, while a reversed polarity was observed in diseased kidney tissues (Fig. 4E–H).

Function of 3D tissue systems in vitro

Although the structures constituted characteristic protein distribution as in native kidney tissues, it is essential to confirm function to have a usable and relevant model for the tissue. The function of the systems was assessed based on transport phenomenon in the cells, since kidney function for the secretion of waste products from blood is mediated by the regulated transport of solutes. Other functions related to the kidney, such as the rennin-angiotensin-aldosterone system, are altered in ADPKD; however, this function involves other organs.[24] Kidney tubules are known to efflux several organic compounds such as antibiotics and pharmacological agents through specific transporters such as OAT genes.[25] This property of kidney tubules was used as a tool to evaluate the function of the structures in the present system. Although there are no reports available for OAT activity in MEK cells, our gene expression data indicate that OAT1 and OAT2 are expressed in diseased cells while OAT2 and OAT3 are expressed in normal cells (data not shown). Organic anion, 6-CF, and PI were used, with the PI included to differentiate dead

cells from live cells and to evaluate whether the uptake of dye was selective for 6-CF alone (Fig. 5A–L). Mutually exclusive staining was seen for 6-CF and PI. Moreover, it was evident that the cellular uptake of 6-CF was limited to live cells and was sensitive to probenecid, an OAT inhibitor (Fig. 5D–F, J–L), in both normal and disease cells in the 3D systems.

3D Tissue in vitro *sustainability*

The sustainability of epithelial tissue structures for longer time periods *in vitro* is a chronic problem in the field of tissue engineering.[26] For example, in the present static system the 3D structures started to collapse after 3 weeks of culture, and the viability of cells was reduced over time (Fig. 6B), attributed to a lack of efficient mass transfer. The possibility of sustaining these cultures for longer time periods was evaluated using a perfusion bioreactor system.[27] A schematic representation of the stepwise procedure for sustaining culture using the perfusion system is shown in Figure 6A. The organization of MEK cells in the 3D aqueous silk fibroin scaffolds with perfusion conditions was analyzed with either matrigel or collagen–matrigel within the 3D porous silk

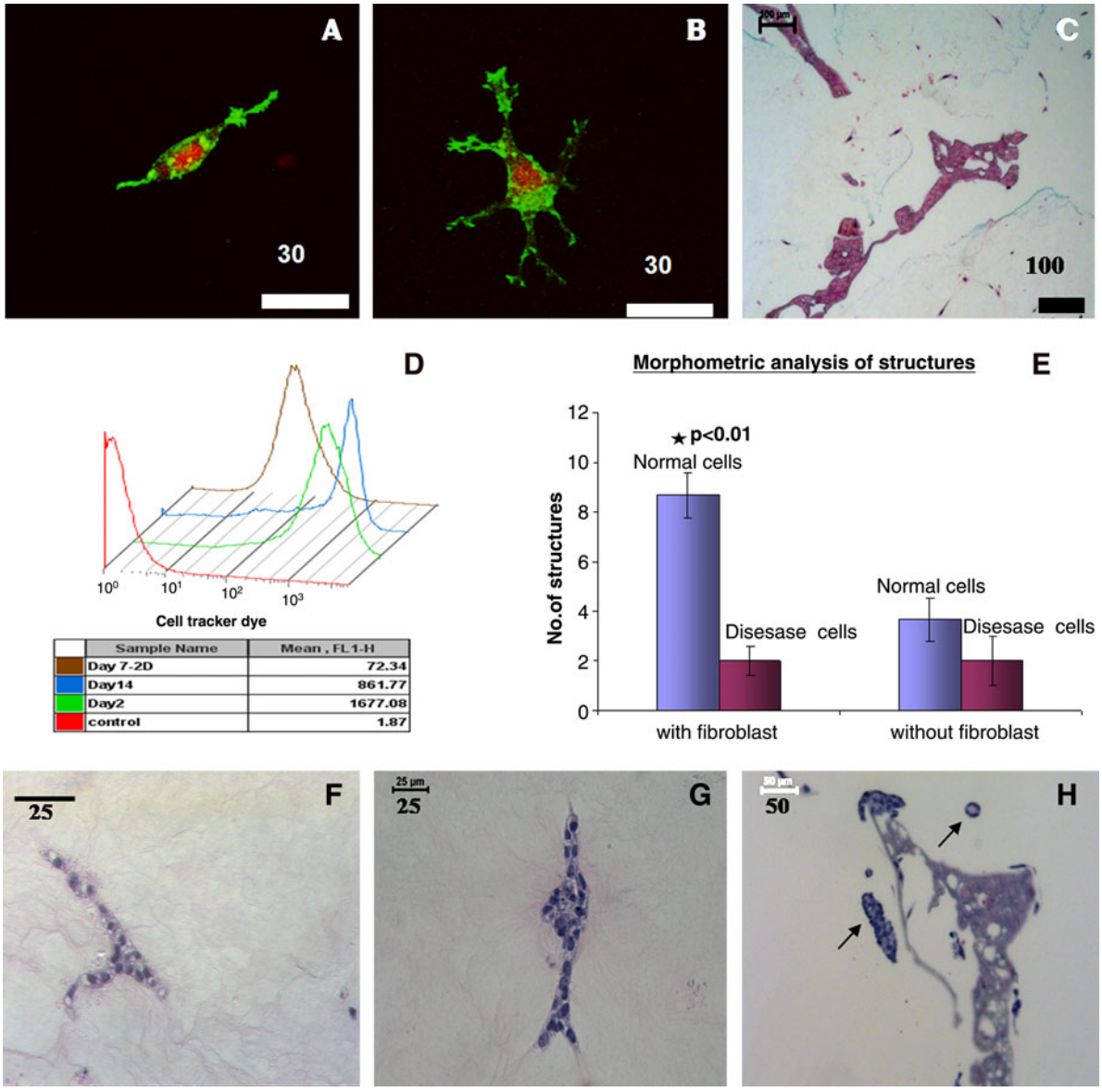

FIG. 2. Characterization of fibroblasts and evaluation of cocultures in collagen–matrigel-infused scaffolds. (**A–D**) Fibroblasts. (**A, B**) Cells were stained for F-actin (green, phalloidin-alexa 488) and nucleus (red, propidium iodide). (**A**) Fibroblast with bipolar morphology. (**B**) Fibroblasts with dendritic extensions. (**C**) H&E image of scaffold with fibroblasts. (**D**) Flow cytometry analysis of fibroblasts showing minimal proliferation. (**E–H**) Evaluation of coculture in collagen–matrigel-infused scaffolds. (**E**) Morphometric analysis of branching/tubular structures in coculture. Significance was seen at $p < 0.01$ between normal cells with fibroblasts and any other groups. Values are in mean ± standard error of the mean. (**F–H**) H&E images of structures observed in coculture. (**F**) Branching structure observed in normal cells. (**G**) A developing tubule structure with bilateral epithelial cells observed in normal cells. (**H**) Cystic and tubule structure observed for disease cells. A tubule and cystic structure developed from disease cells is pointed out in the image. Scale bar in μm. $^*p < 0.01$. Color images available online at www.liebertonline.com/ten.

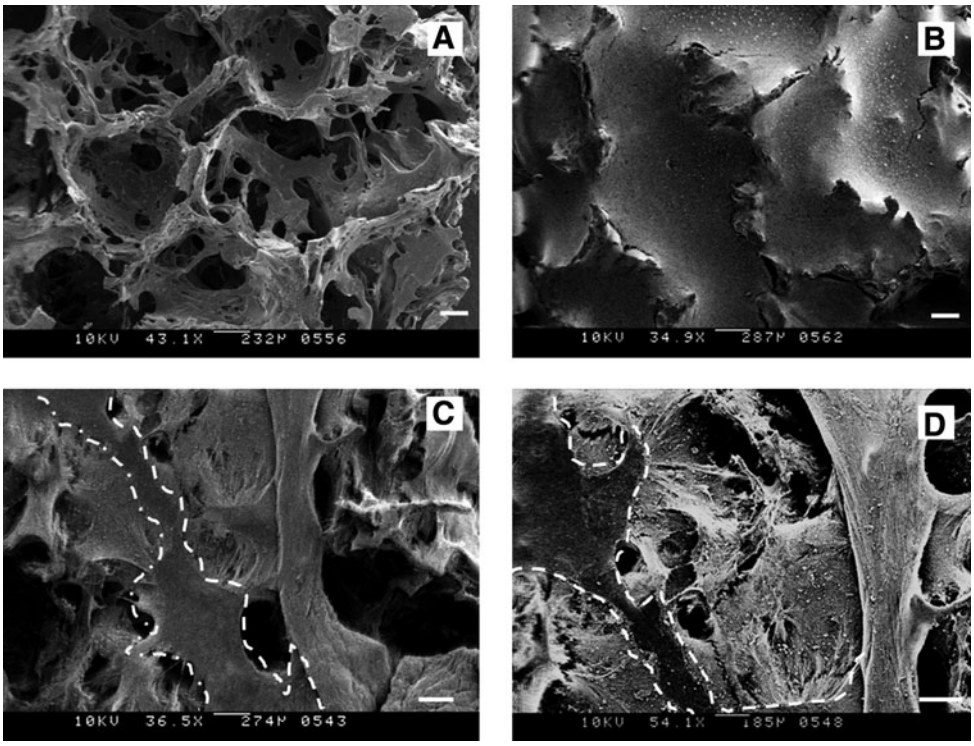

FIG. 3. Morphology characterization of scaffolds. (**A–D**) Scanning electron microscopy images. (**A**) Blank scaffold. (**B**) Collagen–matrigel-infused scaffold without cells. (**C, D**) Collagen–matrigel-infused scaffolds with cells. (**C**) Collagen–matrigel-infused scaffolds with disease cells. (**D**) Collagen–matrigel-infused scaffolds with normal cells. Silk scaffolds region was highlighted in the images (**C**) and (**D**). Scale bar = 200 μm.

scaffolds. The sustainability of the cultures was evaluated with a flow rate of 0.3 mL/min (linear velocity across the matrix 71.8 μm/s), based on other tissue systems.[28] Quantification of structures observed in coculture for perfusion culture indicates that more structures were formed. This may have resulted from enhanced viability of cells in the scaffolds for longer time periods in perfusion culture due to the improved transport. Hematoxylin and eosin and immunofluorescence staining for cell/tissue organization confirmed the sustained formation of structures with structural integrity similar to those in static cultures at 2 weeks (Fig. 6C–J). The structures were sustained for at least 4 weeks in perfusion conditions for the matrigel-infused scaffolds and 6 weeks for the collagen–matrigel-infused coculture scaffolds in comparison with 2 weeks for static culture (Figs. 1 and 2F–H).

Discussion

We present a novel strategy for culturing tubule and ADPKD cyst-derived kidney cells in 3D that is sustainable

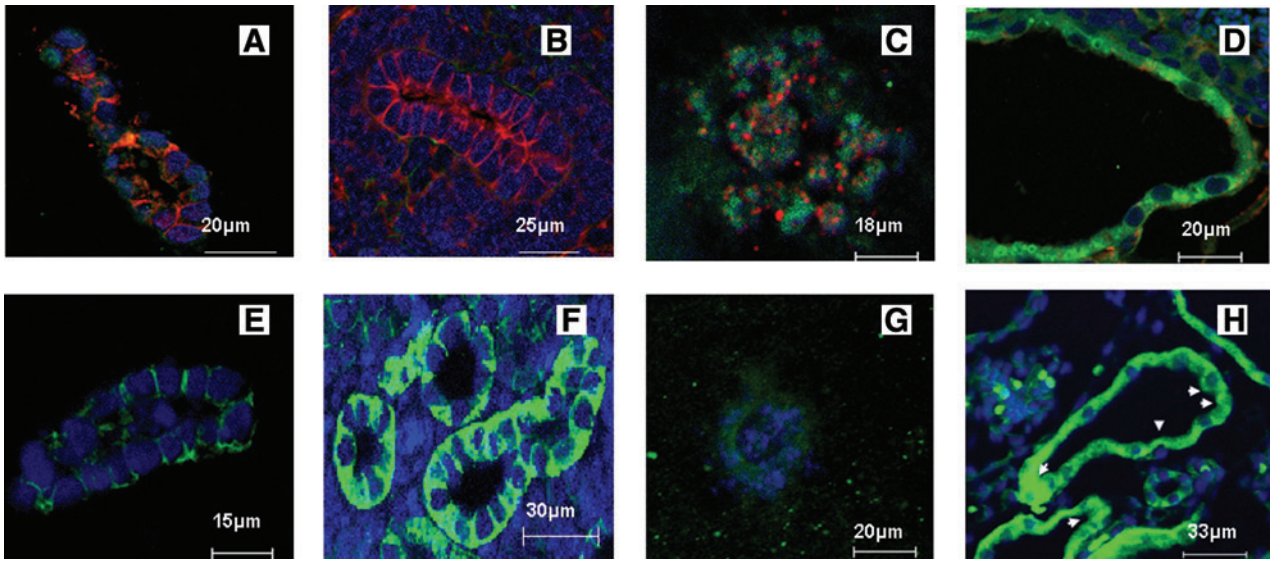

FIG. 4. Evaluation of marker proteins in structures developed in scaffolds. (**A–H**) Immunofluorescence of cells stained for specific markers from paraffin sections. (**A–D**) Cells were stained for E-cadherin (red), N-cadherin (green), and nucleus (blue). (**A**) Normal cells. (**B**) Normal kidney. (**C**) Disease cells. (**D**) Disease kidney. (**E–H**) Stained for Na^+ K^+ ATPase pump (green) and nucleus (blue). (**E**) Normal cells. (**F**) Normal kidney. (**G**) Disease cells. (**H**) Disease kidney. Arrowheads highlight mislocalization. Scale bar in μm. Color images available online at www.liebertonline.com/ten.

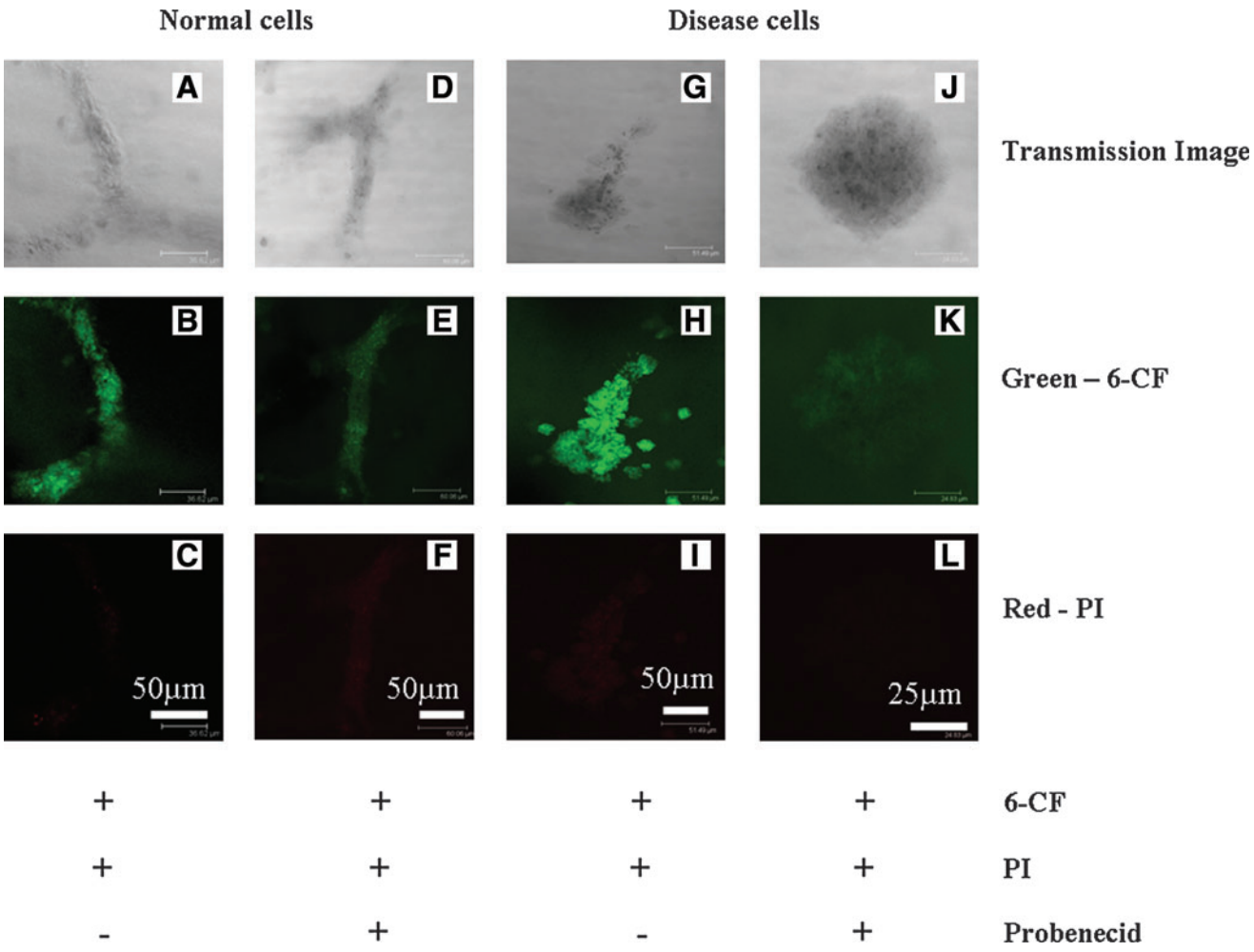

FIG. 5. Organic anion transport in structures developed in scaffolds (**A–L**). Confocal images of whole scaffold imaging for 6-carboxy fluorescein (6-CF) and propidium iodide (PI). (**A–F**) Normal cells. (**G–L**) Disease cells. (**A–C**) Normal cells incubated without probenecid. (**D–F**) Normal cells incubated with probenecid. (**G–I**) Disease cells without probenecid. (**J–L**) Disease cells with probenecid. Scale bar in µm. Color images available online at www.liebertonline.com/ten.

for longer time periods for potential utility in disease interrogation and in drug screening. Scaffold-based cultures and 3D gel systems have been established as 3D culture models.[29,30] Typically, in scaffold-based cultures, cells, such as stem cells, grow along surfaces and eventually fill the interstices to form 3D structures.[3,31] Whereas 3D gel systems comprising epithelial cells were suspended in matrix molecules.[32] Unlike these tissue models, our strategy of culturing cells in matrix molecules infused into sustainable scaffolds provide both complexity and cell signaling benefits exhibited by ECM molecules and the required structural support for extending the systems into bioreactor systems. Moreover, the inclusion of reactor system would allow sustaining the tissue for longer time periods. Synthetic polymers such as polylactic acid have been used for scaffold-based culture models.[33,34] However, degradation lifetimes, inflammatory hydrolytic degradation products, and issues of mechanical strength can impact and modulate the morphogenesis of epithelial cells.[35,36] The composition and state (polymerized vs. denatured) of ECM molecules, such as collagen or matrigel, can also regulate the homeostasis of tissues.[37] Given these features, our strategy employed silk-based scaffolds that are known to be biocompatible, degrade *in vivo* in weeks to years depending on processing, and offer a versatile biomaterial scaffold platform to control structure, morphology, and chemistry, while infusible with ECM components as in the present study.[38]

In the present study, ECM components compatible with silk scaffolds and important for the morphogenesis of MEK cells were studied. The matrix experiments imply that the ECM molecules retained their properties to mediate the morphogenesis of the cells when infused into the porous silk scaffolds. Further, the combination of both collagen and matrigel facilitated the morphogenesis and function of both normal and disease cells and provide a platform to include other cell types. These experiments suggest that surrounding matrix molecules play a crucial role in determining the tissue-related features of cells in our system, while the porous scaffolds provided structural support as well as transport requirements to maintain cell functions. The lack of branching morphogenesis in the disease cells with the collagen–matrigel-infused matrices implicates the essential role of polycystin-1 in morphogenesis of kidney epithelial cells as reported previously.[39]

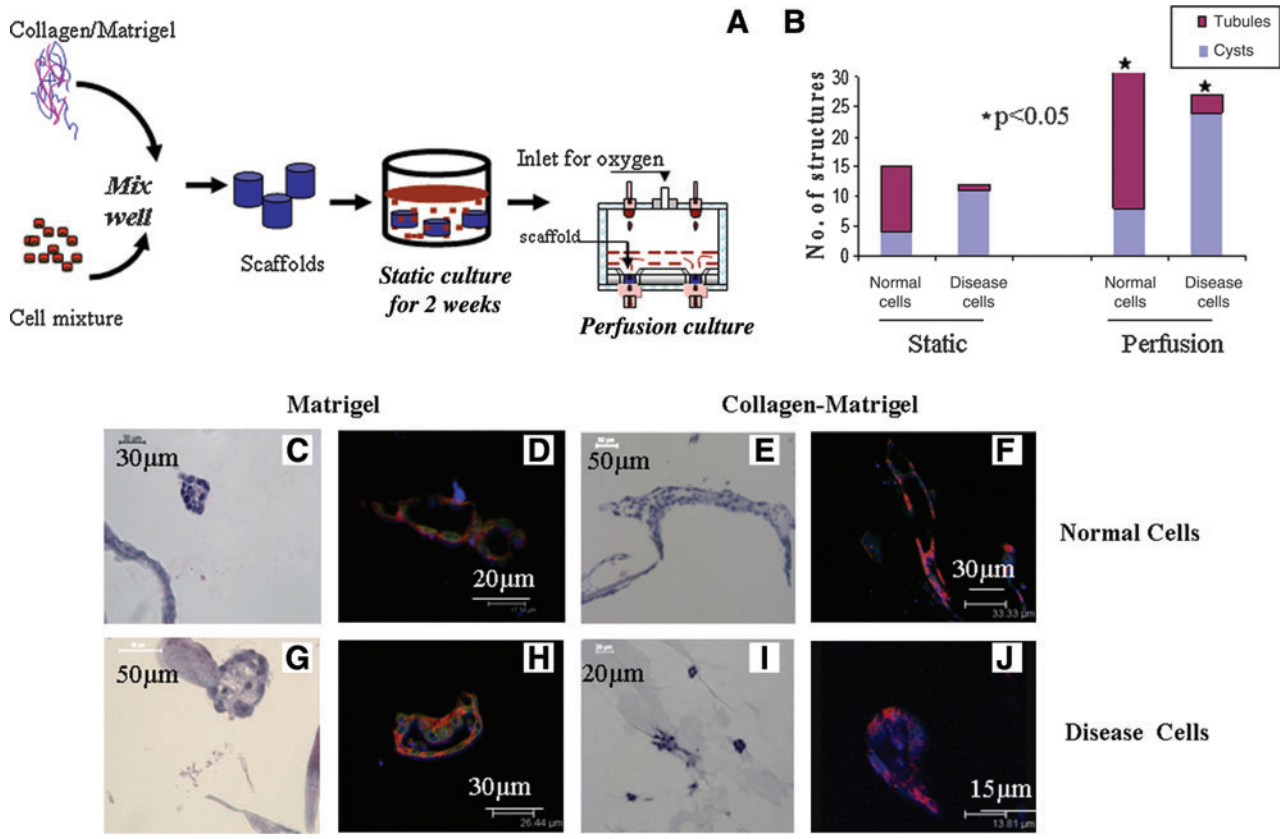

FIG. 6. Sustainability of structures using perfusion bioreactor. (**A**) Schematic representation of stepwise procedure for emulating kidney tissues in scaffolds. (**B**) Quantification of structures observed in coculture conditions in static and perfusion cultures. Culture time was 6 weeks. Average value of structures (cyst and tubules) counted from three sections of each scaffolds (totally four scaffolds) was plotted. Significance was at $p < 0.05$ between static and perfusion culture. (**C–F**) Normal cells. (**G–J**) Disease cells. (**C, E, G, I**) H&E images of scaffold from perfusion culture. (**D, F, H, J**) Immunofluorescence staining for marker proteins E-cadherin (red), N-cadherin (green), and nucleus (blue). (**C, D, G, H**) Matrigel-infused matrix and cultured with epithelial cells alone. Total culture time 4 weeks. (**E, F, I, J**) Collagen–matrigel-infused matrix and cocultured with fibroblasts. Total culture time 6 weeks. Scale bar in µm. *$p<0.05$. Color images available online at www.liebertonline.com/ten.

We have also cocultured MEK cells with fibroblasts and provided a platform to evaluate complex intercellular interactions in kidney-like tissue. Earlier reports with a low seeding density of fibroblast showed procontractile or promigratory phenotype related to the tensile state of 3D collagen matrices.[40,41] Other related studies suggest that local matrix modeling is associated with diverse morphology of fibroblasts as opposed to global matrix modeling such as matrix contraction.[42,43] Moreover, fibroblast proliferation is known to be inhibited by polymerized collagen matrices and growth factor secretions such as HGF modulate the branching morphogenesis of epithelial cells.[44,45] In accordance with these reports, the fibroblasts in the present collagen–matrigel-infused scaffolds exhibited both promigratory and bipolar morphology, and were minimally proliferative. In addition, an increase in branching or tubular structures observed in coculture studies as opposed to single-cell-type culture systems for normal cells indicates possible growth factor secretion from fibroblasts in matrices. Local matrix remodeling was also stimulated as opposed to global matrix contraction that is commonly observed in other 3D gel systems. This was further supported from the SEM characterization of scaffolds, which shows matrix remodeling within the interstices but unaltered integration with the silk scaffolds. These results imply that the cells were cultured in a low tensile strength matrix (collagen–matrigel) with other mechanical cues and growth factor concentration gradients present, similar to *in vivo* conditions.

Epithelial tissues exhibit asymmetric assembly with an apical domain toward the lumen and a basolateral domain to the side of cells and matrix. This asymmetric assembly is mediated by cell–cell and cell–matrix interactions. Cadherins, calcium-dependent adhesion molecules, regulate the cell–cell adhesions and have been widely used as marker proteins for evaluating cell–cell adherence junctions.[46] E-cadherin, a cadherin family member, is basolaterally localized in epithelial cells and regulates cell–cell adhesion. Another cadherin family member, N-cadherin, is usually weakly diffused in the cytoplasm of epithelial cells. A reverse of this feature has been observed in cell–cell adherence junctions in ADPKD.[1,6] The Na^+ K^+ ATPase pump, which exhibits a basolateral distribution similar to E-cadherin, is also mis-localized to apical domains in diseased kidney.[21] Given these characteristics for normal and diseased conditions, we utilized these features to confirm the structural features of the developed tissues. We observed the asym-

metric assembly of normal cells with regard to all three proteins, while protein abnormalities associated with ADPKD were observed for E-cadherin but not for N-cadherin and the Na^+ K^+ ATPase pump. Although speculative, the membrane localization of N-cadherin, reversed polarity for Na^+ K^+ ATPase pump in the diseased kidney, would have been a downstream effect in pathology that could mediate cyst integrity and enlargement. Further, earlier studies from 3D collagen gel systems found cyst enlargement only from heterogeneous cultures of primary cells treated with cyclic adenosine monophosphate (cAMP) elevating agents, such as forskolin.[20] As we are primarily interested in emulating kidney tissues by providing *in vivo*-like conditions, we have not opted for additional supplements such as cAMP-elevating agents. However, our results indicate that there could be additional factors in downstream pathogenesis that cause cyst expansion as observed in kidney tissues. Moreover, the structures we emulated are similar to the ones developed in 3D gel systems and provide a platform to investigate the gene function and decipher the additional factors necessary to mimic the manifestations observed in diseased kidney tissue. Besides asymmetry, we have also shown that our structures are functionally relevant to kidney tissue, based on the ability of the cells to selectively efflux organic anion, 6-CF, and sensitivity to the OAT inhibitor, probenecid. We characterized function using OAT phenomenon, as kidney function for secretion of waste products from blood is mediated by regulated transport of solutes. Earlier studies aimed at reconstitution of kidney development have also shown functional capacity of tubules based on the uptake of organic anions.[41] However, proximal tubular segments are known to be prominent in OAT system activity and it is unclear whether cells from other segments are also capable of such functions. In a study investigating the OAT and organic cationic transport system during embryonic kidney development, collecting duct cells have been shown to uptake organic anions.[47]

Provided with *in vivo*-like emulation of structural and functional features, we have shown the extension of cultures from static to continuous bioreactor systems and thereby sustained these 3D cultures for longer time periods (several weeks). Other approaches involving reactor systems or organotypic cultures have also been reported for kidney tissues.[48,49] However, they lack either the ECM-rich microenvironment to emulate *in vivo* conditions or are not sustainable for longer time periods—at least weeks if not months. Hollow fiber reactor systems have been developed to mimic renal tubular segments and have been used as renal tubule assisting devices.[50] Strategies based on hollow fiber reactors provide optimal transport and other tubule functions, and the fixed fiber diameters limit cyst diameter and would not be relevant for assessing conditions similar to ADPKD, where tubules are transformed into progressive cysts. In contrast, 3D gel systems provide the flexibility to recapitulate enlarging cysts, but are not sustainable for longer time periods due to contraction and loss of transport during degradation. Unlike these systems, our strategy of culturing cells in matrix-infused slow degrading scaffolds would provide conditions to emulate enlarging cyst and can be maintained in dynamic perfusion cultures for extended time frames. Moreover, the use of collagen–matrigel in the system allows cocultures to be generated, adding to the unique attributes for these tissue systems in contrast to other systems reported previously.[18]

The results presented here indicate that the kidney structures were sustainable at least till 6 weeks in perfusion conditions. This is a first important step toward the generation of such sustainable cultures, leading to concepts of studying the formation and progression of the disease, and conducting on-line drug screening. The present studies were conducted with a higher flow rate than typically found in interstitial fluid flow. This was done to ensure that perfusion conditions were provided for cells to grow in scaffolds for longer time periods. While flow-induced stress may be an issue to consider, we suggest that the successful formation of structures and functions of relevance to kidney tissues, with differences observed between normal and diseased cell sources, implies that the conditions were suitable for the intent of the study. The flow rate could be further optimized, and also employed as a tool to examine the impact of flow rate on cell function and kidney tissue function, further extending the utility of the system.

Conclusions

Kidney tissue models developed with ECM-infused scaffolds supported cellular interactions that mimic aspects of kidney tissue morphology and function. Thus, these systems offer a new option for tissue study that can provide benefits for the systematic analysis of disease and for therapeutic screening. The methodology adapted provides control over two essential parameters for ADPKD that cannot be obtained in other systems. (1) Structures can be grown without any dimensional confinement in the pores of the scaffolds. (2) Perfusion of media supports sustainable structures for longer time periods, allowing investigations for longer time periods and the accommodation of multiple cell types. Moreover, the guidelines given here could be applied to establish human kidney tissue models or other epithelial organs.

Acknowledgments

The authors would like to thank Leah Contrino from Renal Division, Brigham and Women's Hospital, for preparation of kidney samples. Further, we appreciate the technical guidance from Catherine Linsenmayer from Tufts School of Medicine for SEM analysis. The research was supported by Genzyme GRIP program and NIH Tissue Engineering Resource Center (P41 EB002520) for DLK and ROI DK40703, R37DK51050 for J.Z.

Disclosure Statement

No competing financial interests exist.

References

1. Bryant, D., and Mostov, K. From cells to organs: building polarized tissue. Nat Rev Mol Cell Biol **9,** 887, 2008.
2. Patwari, P., and Lee, R.T. Mechanical control of tissue morphogenesis. Circ Res **103,** 234, 2008.
3. Kim, J.B. Three dimensional tissue culture models in cancer biology. Semin Cancer Biol **15,** 365, 2005.
4. Yamada, K., and Cukierman, E. Modeling tissue morphogenesis and cancer in 3D. Cell **130,** 601, 2007.
5. Griffith, L.G., and Swartz, M.A. Capturing complex 3D tissue physiology *in vitro*. Nat Rev Mol Cell Biol **7,** 211, 2006.

6. Torres, V.E., and Harris, P.C. Mechanism of disease: autosomal dominant and recessive polycystic kidney disease. Nat Clin Pract Nephrol **2,** 40, 2006.
7. Torres, V.E., Harris, P.C., and Prison, Y. Autosomal dominant polycystic kidney disease. Lancet **369,** 1287, 2007.
8. Li, X., Luo, Y., Starremans, P.G., McNamara, C.A., Pei, Y., and Zhou, J. Polycystin-1 and polycystin-2 regulate the cell cycle through the helix-loop-helix inhibitor Id2. Nat Cell Biol **7,** 1202, 2005.
9. Nauli, S.M., Alenghat, F.J., Luo, Y., Williams, E., Vassilev, P., Li, X., Elia, A.E., Lu, W., Brown, E.M., Quinn, S.J., Ingber, D.E., and Zhou, J. Polycystins 1 and 2 mediate mechanosensation in the primary cilium of kidney cells. Nat Genet **33,** 129, 2003.
10. Boca, M., D'Amato, L., Distefano, G., Polishchuk, R.S., Germino, G.G., and Boletta, A. Polycystin-1 induces cell migration by regulating phosphatidylinositol 3-kinase-dependent cytoskeletal rearrangements and GSK3beta-dependent cell-cell mechanical adhesion. Mol Biol Cell **18,** 4050, 2007.
11. Shillingford, J.M., Murcia, N.S., Larson, C.H., Low, S.H., Hedgepeth, R., Brown, N., Flask, C.A., Novick, A.C., Goldfarb, D.A., Kramer-Zucker, A., Walz, G., Piontek, K.B., Germino, G.G., and Weimbs, T. The mTOR pathway is regulated by polycystin-1, and its inhibition reverses renal cystogenesis in polycystic kidney disease. Proc Natl Acad Sci USA **103,** 5466, 2006.
12. Lal, M., Song, X., Pluznick, J.L., Di Giovanni, V., Merrick, D.M., Rosenblum, N.D., Chauvet, V., Gottardi, C.J., Pei, Y., and Caplan, M.J. Polycystin-1 C-terminal tail associates with beta-catenin and inhibits canonical Wnt signaling. Hum Mol Genet **17,** 3105, 2008.
13. Nauli, S.M., Rossetti, S., Kolb, R.J., Alenghat, F.J., Consugar, M.B., Harris, P.C., Ingber, D.E., Loghman-Adham, M., and Zhou, J. Loss of polycystin-1 in human cyst lining epithelia leads to ciliary dysfunction. J Am Soc Nephrol **17,** 1015, 2006.
14. Shimazu, K., Toda, S., Miyazono, M., Sakemi, T., and Sugihara, H. Morphogenesis of MDCK cells in a collagen gel matrix culture under stromal adipocyte-epithelial cell interaction. Kidney Int **60,** 568, 2001.
15. Okada, H., Ban, S., Nagao, S., Takahashi, H., Suzuki, H., and Neilson, E.G. Progressive renal fibrosis in murine polycystic kidney disease: an immunohistochemical observation. Kidney Int **58,** 58, 2000.
16. Wilson, P.D. Mouse models of polycystic kidney disease. Curr Top Dev Biol **84,** 311, 2008.
17. Pampaloni, F., Reynaud, E.G., and Stelzer, E.H. The third dimension bridges the gap between cell culture and live tissue. Nat Rev Mol Cell Biol **8,** 839, 2007.
18. Altman, G.H., Diaz, F., Jakuba, C., Calabro, T., Horan, R.L., Chen, J., Lu, H., Richmond, J., and Kaplan, D.L. Silk-based biomaterials. Biomaterials **24,** 401, 2003.
19. Kim, H.J., Kim, U.J., Kim, H.S., Li, C., Wada, M., Leisk, G.G., and Kaplan, D.L. Bone tissue engineering with premineralized silk scaffolds. Bone **42,** 1226, 2008.
20. Hanaoka, K., and Guggino, W.B. cAMP regulates cell proliferation and cyst formation in autosomal polycystic kidney disease cells. J Am Soc Nephrol **11,** 1179, 2000.
21. Carone, F.A., Nakamura, S., Bacallao, R., Nelson, W.J., Khokha, M., and Kanwar, Y.S. Impaired tubulogenesis of cyst-derived cells from autosomal dominant polycystic kidneys. Kidney Int **47,** 861, 1995.
22. Leroy, P., and Mostov, K.E. Slug is required for cell survival during partial epithelial-mesenchymal transition of HGF-induced tubulogenesis. Mol Biol Cell **18,** 1943, 2007.
23. Daley, W.P., Peters, S.B., and Larsen, M. Extracellular matrix dynamics in development and regenerative medicine. J Cell Sci **121,** 255, 2008.
24. Schrier, R.W. Renal volume, renin-angiotensin-aldosterone system, hypertension, and left ventricular hypertrophy in patients with autosomal dominant polycystic kidney disease. J Am Soc Nephrol **20,** 1888, 2009.
25. Wright, S.H., and Dantzler, W.H. Molecular and cellular physiology of renal organic cation and anion transport. Physiol Rev **84,** 987, 2004.
26. Minuth, W.W., Sittinger, M., and Kloth, S. Tissue engineering: generation of differentiated artificial tissues for biomedical applications. Cell Tissue Res **29,** 1, 1998
27. Fröhlich, M., Grayson, W.L., Marolt, D., Gimble, J.M., Kregar-Velikonja, N., and Vunjak-Novakovic, G. Bone grafts engineered from human adipose-derived stem cells in perfusion bioreactor culture. Tissue Eng Part A **16,** 179, 2010.
28. Grayson, W.L., Bhumiratana, S., Cannizzaro, C., Chao, P.H., Lennon, D.P., Caplan, A.I., and Vunjak-Novakovic, G. Effects of initial seeding density and fluid perfusion rate on formation of tissue-engineered bone. Tissue Eng Part A **14,** 1809, 2008.
29. Fischbach, C., Chen, R., Matsumoto, T., Schmelzle, T., Brugge, J.S., Polverini, P.J., and Mooney, D.J. Engineering tumors with 3D scaffolds. Nat Methods **4,** 855, 2007.
30. Debnath, J., and Brugge, J.S. Modelling glandular epithelial cancers in three-dimensional cultures. Nat Rev Cancer **5,** 675, 2005.
31. Wang, Y., Kim, U.J., Blasioli, D.J., Kim, H.J., and Kaplan, D.L. *In vitro* cartilage tissue engineering with 3D porous aqueous-derived silk scaffolds and mesenchymal stem cells. Biomaterials **26,** 7082, 2005.
32. Elberg, G., Guruswamy, S., Logan, C.J., Chen, L., and Turman, M.A. Plasticity of epithelial cells derived from human normal and ADPKD kidneys in primary cultures. Cell Tissue Res **331,** 495, 2008.
33. Evans, G.R., Brandt, K., Katz, S., Chauvin, P., Otto, L., Bogle, M., Wang, B., Meszlenyi, R.K., Lu, L., Mikos, A.G., and Patrick, C.W. Jr. Bioactive poly(L-lactic acid) conduits seeded with Schwann cells for peripheral nerve regeneration. Biomaterials **23,** 841, 2002.
34. Rezwan, K., Chen, Q.Z., Blaker, J.J., and Boccaccini, A.R. Biodegradable and bioactive porous polymer/inorganic composite scaffolds for bone tissue engineering. Biomaterials **27,** 3413, 2006.
35. Paszek, M.J., Zahir, N., Johnson, K.R., Lakins, J.N., Rozenberg, G.I., Gefen, A., Reinhart-King, C.A., Margulies, S.S., Dembo, M., Boettiger, D., Hammer, D.A., and Weaver, V.M. Tensional homeostasis and the malignant phenotype. Cancer Cell **8,** 241, 2005.
36. Rosines, E., Schmidt, H.J., and Nigam, S.K. The effect of hyaluronic acid size and concentration on branching morphogenesis and tubule differentiation in developing kidney culture systems: potential applications to engineering of renal tissues. Biomaterials **28,** 4806, 2007.
37. Egles, C., Shamis, Y., Mauney, J.R., Volloch, V., Kaplan, D.L., and Garlick, J.A. Denatured collagen modulates the phenotype of normal and wounded human skin equivalents. J Invest Dermatol **128,** 1830, 2008
38. Wang, Y., Rudym, D.D., Walsh, A., Abrahamsen, L., Kim, H.J., Kim, H.S., Kirker-Head, C., and Kaplan, D.L. *In vivo* degradation of three-dimensional silk fibroin scaffolds. Biomaterials **29,** 3415, 2008.

39. Nickel, C., Benzing, T., Sellin, L., Gerke, P., Karihaloo, A., Liu, Z.X., Cantley, L.G., and Walz, G. The polycystin-1 C-terminal fragment triggers branching morphogenesis and migration of tubular kidney epithelial cells. J Clin Invest **9,** 481, 2002.
40. Rhee, S., and Grinnell, F. Fibroblast mechanics in 3D collagen matrices. Adv Drug Deliv Rev **59,** 1299, 2007.
41. Grinnell, F., Ho, C.H., Tamariz, E., Lee, D.J., and Skuta, G. Dendritic fibroblasts in three-dimensional collagen matrices. Mol Biol Cell **14,** 384, 2003.
42. Tamariz, E., and Grinnell, F. Modulation of fibroblast morphology and adhesion during collagen matrix remodeling. Mol Biol Cell **13,** 3915, 2002.
43. Xia, H., Nho, R., Kleidon, J., Kahm, J., and Henke, C.A. Polymerized collagen inhibits fibroblast proliferation via a mechanism involving the formation of a beta1 integrin-protein phosphatase 2A-tuberous sclerosis complex 2 complex that suppresses S6K1 activity. J Biol Chem **283,** 20350, 2008.
44. Montesano, R., Matsumoto, K., Nakamura, T., and Orci, L. Identification of a fibroblast-derived epithelial morphogen as hepatocyte growth factor. Cell **29,** 901, 1991.
45. Rosines, E., Sampogna, R.V., Johkura, K., Vaughn, D.A., Choi, Y., Sakurai, H., Shah, M.M., and Nigam, S.K. Staged *in vitro* reconstitution and implantation of engineered rat kidney tissue. Proc Natl Acad Sci USA **104,** 20938, 2007.
46. Okada, T.S. The expression of cell adhesion molecules, cadherins: markers of kidney morphogenesis. Pediatr Nephrol **2,** 115, 1988.
47. Sweet, D.H., Eraly, S.A., Vaughn, D.A., Bush, K.T., and Nigam, S.K. Organic anion and cation transporter expression and function during embryonic kidney development and in organ culture models. Kidney Int **69,** 837, 2006.
48. Saxén, L., and Lehtonen, E. Embryonic kidney in organ culture. Differentiation **36,** 2, 1987.
49. Iwahori, T., Matsuno, N., Johjima, Y., Konno, O., Akashi, I., Nakamura, Y., Hama, K., Iwamoto, H., Uchiyama, M., Ashizawa, T., and Nagao, T. Radial flow bioreactor for the creation of bioartificial liver and kidney. Transplant Proc **37,** 212, 2005.
50. Humes, H.D., MacKay, S.M., Funke, A.J., and Buffington, D.A. Tissue engineering of a bioartificial renal tubule assist device: *in vitro* transport and metabolic characteristics. Kidney Int **55,** 2502, 1999.

Address correspondence to:
David L. Kaplan, Ph.D.
Department of Biomedical Engineering
Tufts University
4 Colby St.
Medford, MA 02155

E-mail: david.kaplan@tufts.edu.

Received: September 3, 2009
Accepted: April 20, 2010
Online Publication Date: June 8, 2010